bioRxiv preprint doi: https://doi.org/10.1101/2021.12.07.471485; this version posted December 9, 2021. The copyright holder for this preprint (which was not certified by peer review) is the author/funder, who has granted bioRxiv a license to display the preprint in perpetuity. It is made available under aCC-BY-NC-ND 4.0 International license.

Small transcriptional differences lead to distinct NF-κB dynamics in quasi-identical cells

Cise Kizilirmak[1,2], Emanuele Monteleone[1,2], Jose M. García-Manteiga[3], Francesca Brambilla[2], Alessandra Agresti[1,2], Marco E. Bianchi[1,2,*] and Samuel Zambrano [1,2,4,*]

[1]School of Medicine, Vita-Salute San Raffaele University, Milan, 20132, Italy.

[2] Division of Genetics and Cell Biology, IRCCS San Raffaele Scientific Institute, Milan, 20132, Italy.

[3] Center for Omics Sciences. IRCCS San Raffaele Scientific Institute, Milan, 20132, Italy.

[4] Lead contact.

[*] Correspondence to: M.E.B: bianchi.marco@hsr.it SZ: zambrano.samuel@hsr.it.

bioRxiv preprint doi: https://doi.org/10.1101/2021.12.07.471485; this version posted December 9, 2021. The copyright holder for this preprint (which was not certified by peer review) is the author/funder, who has granted bioRxiv a license to display the preprint in perpetuity. It is made available under aCC-BY-NC-ND 4.0 International license.

ABSTRACT

Transcription factor dynamics is fundamental to determine the activation of accurate transcriptional programs and yet is heterogeneous at single-cell level. The source of this dynamic variability is not completely understood. Here we focus on the nuclear factor κB (NF-κB), whose dynamics have been reported to cover a wide spectrum ranging from oscillatory to non-oscillatory. We show that clonal populations of immortalized fibroblasts derived from a single mouse embryo (that can hence be considered quasi-identical) display robustly distinct dynamics upon tumor necrosis α (TNF-α) stimulation. Combining transcriptomics, data-constrained mathematical modelling, and mRNA interference we show that small differences in the expression of genes belonging to the NF-κB regulatory circuit are predictive of the distinct responses to inflammatory stimuli observed among the clones. We propose that this transcriptional fine-tuning can be a general mechanism to produce cell subpopulations with distinct dynamic responses to stimuli within homogeneous cell populations.

bioRxiv preprint doi: https://doi.org/10.1101/2021.12.07.471485; this version posted December 9, 2021. The copyright holder for this preprint (which was not certified by peer review) is the author/funder, who has granted bioRxiv a license to display the preprint in perpetuity. It is made available under aCC-BY-NC-ND 4.0 International license.

INTRODUCTION

Cells are able to provide precise transcriptionally-mediated responses to the complex mixture of external and internal stimuli to which they are subjected (Milo and Phillips, 2015). In this context, a key role is played by transcription factors (TFs), proteins that are "activated" upon stimuli and selectively trigger the expression of target genes coding for proteins required for an adequate response. The activation of several TFs is primarily mediated by their nuclear accumulation and is tightly regulated by other players within their genetic regulatory circuit, whose design contributes to providing a specific transcriptional output given a certain input (Alon, 2007). The nuclear accumulation of TFs is dynamic and can be oscillatory, as shown first for circadian rhythms in response to the day/night cycle (Patke et al., 2020) and the cell cycle (Ferrell et al., 2011); oscillations were then discovered for a wide variety of TFs (Levine et al., 2013). The emerging view is that such dynamics is not merely a by-product of the regulatory mechanisms of the TFs, but that it has a functional role in gene expression (Purvis and Lahav, 2013) and impacts a wide array of cellular process, e.g. determining cell fate (as for p53, (Purvis et al., 2012)), the response to mechanical cues (as for YAP/TAZ, (Franklin et al., 2020)) or the speed of the segmentation clock during embryo development (as for Hes7, (Matsuda et al., 2020)). Of note, single cell measures show consistently a high degree of heterogeneity in TF dynamics within a population, which yet is compatible with the TFs' ability to provide an accurate transcriptional output given an input (Selimkhanov et al., 2014).

The NF-κB system is a paradigmatic example of the dynamic nature of TF activation. NF-κB is a family of dimeric TFs that plays a central role in innate and adaptive immune responses (Hayden and Ghosh, 2008; Natoli and Ostuni, 2019); dimers including the monomer p65 have the strongest transcription activating potential (Schmitz and Baeuerle, 1991) and are involved in the canonical pathway (we'll refer to such dimers as NF-κB in what follows). NF-κB is kept in the cytosol bound by its inhibitors IκB, which are degraded upon external inflammatory stimuli such as the cytokine Tumor Necrosis Factor alpha (TNF-α) and are themselves NF-κB transcriptional targets (A.Hoffmann et al., 2002). It was immediately evident and subsequently confirmed by live cell imaging that this system of negative feedbacks could lead to oscillations in the nuclear concentration of NF-κB upon stimulation in single cells (Nelson et al., 2004; Sung et al., 2009; Tay et al., 2010; Zambrano et al., 2014a). NF-κB nuclear localization dynamics (in short, NF-κB dynamics) have the potential to discriminate between ligand dose (Zhang et al., 2017a) and type (Adelaja et al., 2021; Martin et al., 2020) and determines target gene expression (Ashall et al., 2009; Lee et al., 2014; Sung et al., 2009; Tay et al., 2010) in a functionally relevant way (Zambrano et al., 2016). However, terming such dynamics "oscillatory" is somewhat simplistic: a salient feature of all these studies is that the dynamics can be qualitatively quite different between cell types, ranging from sustained oscillations with a period of 1.5 hours for 3T3 cells (Kellogg and Tay, 2015), damped oscillations for mouse embryonic fibroblasts (Zambrano et al., 2016), persistent nuclear localization for RAW or 3T3 cells upon LPS (Lee et al., 2009; Sung et al., 2014) and non-oscillatory for HeLa cells (Lee et al., 2014). Even within a population of cells of the same type individual cells display dynamical heterogeneity and qualitatively different dynamics, with cells that oscillate and cells that do not (Nelson et al., 2004; Zambrano et al., 2014a). The origin of these differences is far from being clear and yet can have important functional consequences, for example in the cell's life-death decisions (Lee et al., 2016) and in its epigenetic state

bioRxiv preprint doi: https://doi.org/10.1101/2021.12.07.471485; this version posted December 9, 2021. The copyright holder for this preprint (which was not certified by peer review) is the author/funder, who has granted bioRxiv a license to display the preprint in perpetuity. It is made available under aCC-BY-NC-ND 4.0 International license.

(Cheng et al., 2021). Understanding the origin of such differences can shed light on how the NF-κB system uses dynamics to produce a desired output given a certain input, and more in general on the mechanisms by which cells within a population produce distinct TF dynamic responses to stimuli.

Here, we focused on immortalized GFP-NF-κB mouse fibroblasts (MEFs) derived from a single embryo. These cells can be considered "quasi-identical": they share the same genome derived from a single individual, albeit with sparse variations accumulated during in vitro cultivation and immortalization. Yet, in these cells qualitatively and quantitatively different dynamics can be observed (De Lorenzi et al., 2009; Sung et al., 2009; Zambrano et al., 2014a, 2016). To determine the origin of such dynamical variations, we isolated several clones and we found that each of them has distinct and clonally heritable NF-κB dynamics upon TNF-α. We focused on three archetypical clones with persistent, oscillatory, and weak responses, respectively. Transcriptomic analysis and mathematical modelling show that small but significant differences in the expression level of key mediators of NF-κB activation are predictive of the strength of the response upon TNF-α as defined by the maximum and/or the area under the curve of the nuclear localization. Likewise, differences in expression levels of the components of the IL-1β signaling pathway predict the distinct NF-κB activation of the clones upon IL-1β stimulation. Furthermore, differences in the expression of the system's negative feedbacks predict the differences in the decay of the activation, i.e., the sharpness of the response. Indeed, interfering with the expression of the repressor IκBα can make cells switch from a sharp response to a more persistent nuclear localization dynamics.

Taken together, our results show that small differences in the expression levels of the genes of the NF-κB regulatory circuit can produce distinct responses in cells of the same type derived from the same organism. This mechanism explains how multicellular organisms can produce diverse cell types with selective and specialized NF-κB-mediated response to inflammatory stimuli.

bioRxiv preprint doi: https://doi.org/10.1101/2021.12.07.471485; this version posted December 9, 2021. The copyright holder for this preprint (which was not certified by peer review) is the author/funder, who has granted bioRxiv a license to display the preprint in perpetuity. It is made available under aCC-BY-NC-ND 4.0 International license.

RESULTS

1. Clonal populations of fibroblasts derived from a single embryo display distinct NF-κB dynamics upon TNF-α

Whereas different dynamics have been reported in different cell types, we decided to focus on quasi-identical cells: immortalized mouse embryonic fibroblasts (MEFs in what follows) derived from a single homozygous GFP-p65 knock-in embryo (see (De Lorenzi et al., 2009) and **Methods**). We challenged our GFP-p65 MEF cell population with 10 ng/ml tumor necrosis factor alpha (TNF-α) and quantified the nuclear to cytosolic intensity of NF-κB (NCI) using our established method of live cell imaging ((Zambrano et al., 2014a, 2016), and **Methods**). As previously reported (De Lorenzi et al., 2009; Sung et al., 2009; Zambrano et al., 2014a, 2016) the response of these MEFs upon TNF-α is heterogeneous (**Figure 1A** and **Movie S1**). Most cells display oscillatory peaks of nuclear localization while others display a non-oscillatory dynamics (**Figure 1B**), a kind of dynamics also referred to as "persistent activation" and similar to the one reported for macrophages (Cheng et al., 2021; Sung et al., 2014) and fibroblasts (Lee et al., 2009) upon lipopolysaccharide (LPS) stimulation. We can indeed analyze NF-κB dynamics of hundreds of cells (see **Methods** and **Figure S1A**) and plot them to form a "dynamic heatmap" (**Figure 1C**), which captures the dynamics across the cell population (**Figure 1C**).

Starting from our original population of MEFs (that we refer to as the "pool" in what follows) we generated 17 clonal populations following standard procedures (**Figure 1D** and **Methods**). Eight clonal population were imaged upon stimulation with 10 ng/ml TNF-α. We found that NF-κB dynamics of each clonal population upon TNF-α was markedly different, even if a certain degree of intra-clonal heterogeneity was observed (**Figure 1E**). To have an unbiased confirmation of this observation, we utilized an unsupervised stochastic clustering approach (see **Methods**), which grouped NF-κB dynamic profiles according to their shapes into 8 different clusters (**Figure S1B**). We then calculated the probability for two profiles to cluster together (**Figure S1C** and **S1D**); the result of many realizations of this stochastic procedure indicates that NF-κB dynamic profiles of cells of the same clone are significantly more likely to cluster together than with profiles of cells of other clones (**Figure 1F**). An entropy-based clustering degree parameter based on these probabilities gives significantly higher value when the profiles are assigned to the proper clonal population than when they are randomly mixed and then stochastically clustered (see **Methods** and **Figure 1G**), further indicating that NF-κB profiles within a clonal population are similar.

In sum, we can isolate clones from a population of MEFs derived from a single embryo that have distinct dynamical behaviors already observed in the original cell population.

bioRxiv preprint doi: https://doi.org/10.1101/2021.12.07.471485; this version posted December 9, 2021. The copyright holder for this preprint (which was not certified by peer review) is the author/funder, who has granted bioRxiv a license to display the preprint in perpetuity. It is made available under aCC-BY-NC-ND 4.0 International license.

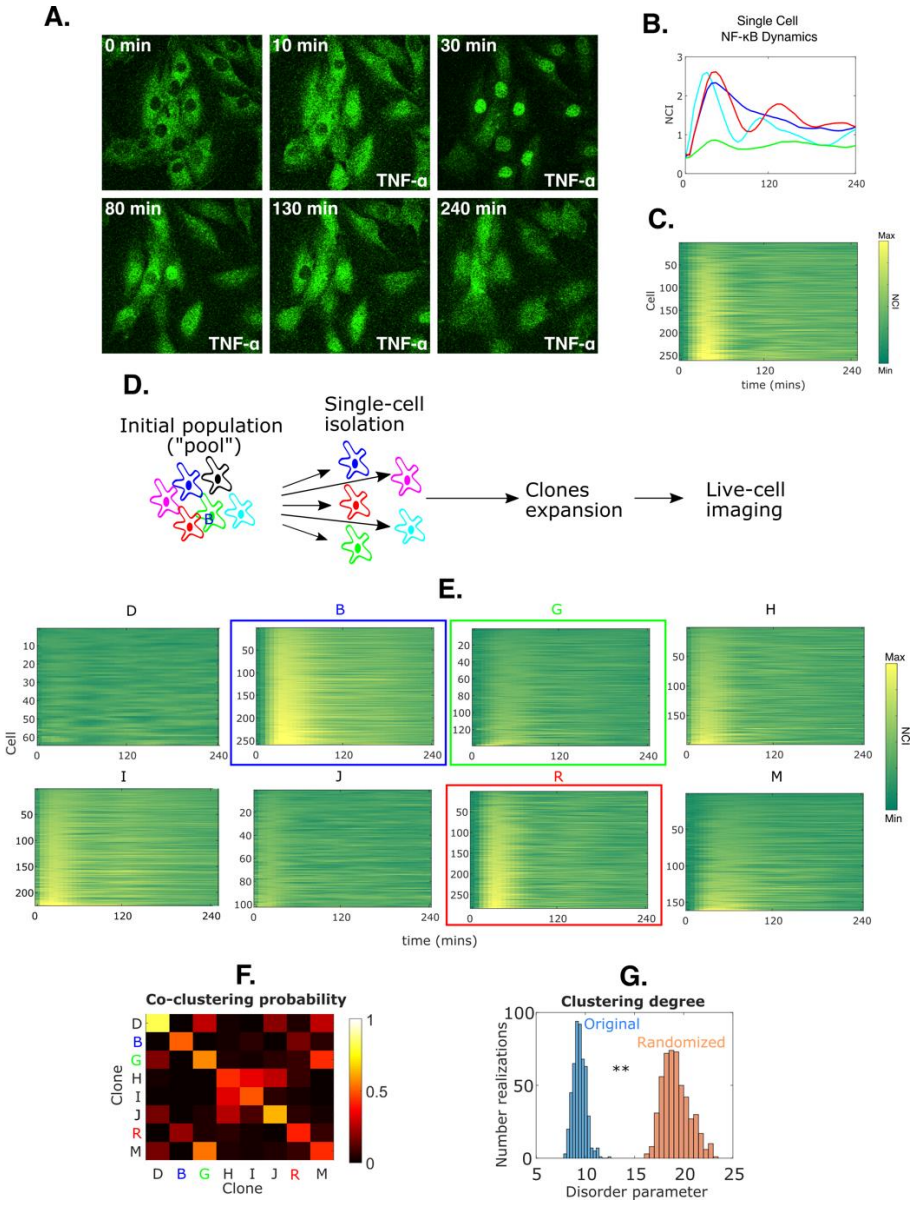

Figure 1. Clonal populations derived from an initial population of MEFs have distinct dynamics upon TNF-α. A. Representative images of the heterogeneous response to 10 ng/ml TNF-α of our initial population of MEFs. **B.** NF-κB dynamic profiles of four randomly selected cells from our population. **C.** The heatmap represents the NF-κB dynamics of hundreds of cells sorted by their maximum NCI value. **D.** Single cell cloning strategy of our initial population of MEFs (referred to as "pool"). Clones were expanded and used for live cell imaging. **E.** Dynamic heatmaps of eight clones isolated from our population (Clones B, R and G are highlighted). **F.** The color-coded plot shows co-clustering probability of NF-κB dynamic profiles between different clones based on an unsupervised k-means clustering. **G.** Distribution of the values of an entropy-like disorder parameter calculated for each realization of the stochastic clustering for the original dataset versus a randomized one. The distributions do not overlap in 500 realizations of the stochastic clustering for the original and the randomized datasets, $p<2\cdot10^{-3}$.

bioRxiv preprint doi: https://doi.org/10.1101/2021.12.07.471485; this version posted December 9, 2021. The copyright holder for this preprint (which was not certified by peer review) is the author/funder, who has granted bioRxiv a license to display the preprint in perpetuity. It is made available under aCC-BY-NC-ND 4.0 International license.

2. NF-κB dynamics and oscillatory behavior of cells is different between clones yet heterogeneous within clonal populations

We then chose 3 clones with archetypical dynamics reminiscent of those observed in the literature and in cells in our original MEF population (**Figure 1B**): a clone with more persistent nuclear localization of NF-κB (clone B, blue), one with a first well-defined sharp peak (clone R, red) (in other words, a nuclear localization that decreases fast (Zambrano et al., 2020)) and a clone characterized by a low activation of NF-κB (clone G, green) (**Figure 1E**).

Clonal populations R, G, and B showed clearly distinct NF-κB dynamics even by direct inspection of their time-lapses (**Figure 2A** and **Movie S2-S4**). The average NF-κB activation profiles (**Figure 2B**) show how NF-κB response is stronger for clone B than for clone R, and for clone R than for clone G (order relation B>R>G). Such differences were strikingly robust across replicated experiments (examples of replicates shown in **Figure S2A**) and were conserved also for higher TNF-α doses (100 ng/ml) (**Figure S2B**). Importantly, these differences were also conserved after many cell divisions and culture passages, even if the average response to TNF-α was weaker for all clones after 8 weeks in culture (**Figure S2C**).

We then investigated cell-to-cell heterogeneity within single clones. The dynamic variability calculated through the coefficient of variation showed that the clones have less variability than the pool, as expected (**Figure S2D**). Next, we focused on classic quantifiers of NF-κB response, such as the height of the first peak, its timing and the area under the curve (AUC) (Tay et al., 2010; Zambrano et al., 2014a). We found that the values of such quantifiers are heterogeneous among cells of the same clone, although the differences are statistically significant between the clones and remarkably similar across replicates (**Figure 2C** and **Figure S2E**). The first peak of activation is typically higher for cells of clone B than for cells of clone R, which in turn have much higher peaks than cells of clone G (**Figure 2C**), so the B>R>G relation is preserved at single cell level. Interestingly, clone G has the lower peak value in spite of having the higher basal levels of nuclear NF-κB (**Figure S2F**), so the resulting fold change of nuclear NF-κB upon TNF-α, a key factor for gene expression (Lee et al., 2014), is also different across the clonal populations. The timing of the first peak is equally prompt within our experimental resolution in clones B and R, but slightly slower in clone G (**Figure 2C**). The larger differences though are observed in the area under the curve (**Figure 2C**), which is much higher for clone B than for clone R, and is again the lowest for clone G. This captures well our observation that clone B has a more persistent NF-κB nuclear localization dynamics, while clone R displays a sharper response. We did also verify that all the differences above hold true when considering the absolute intensity of the nuclear signal (**Figure S2G**) instead of the nuclear to cytosolic intensity of NF-κB, and also when we manually segmented the cells' nuclei (**Figure S2H**).

The differences between clonal populations could be related to intrinsic or extrinsic factors such as cell cycle, which has been already shown to modulate the response to TNF-α (Ankers et al., 2016). Thus, we compared the cell cycle distributions of our populations (see **Methods**, **Figure S2I** and **Table S1**). Clone B and Clone G have very similar distributions, but they display the clearest differences in the dynamics of NF-κB response, suggesting that the cell cycle has a limited impact on their inter-clonal dynamic differences. Clones B and R are slightly more different, so we applied a computational correction for the

bioRxiv preprint doi: https://doi.org/10.1101/2021.12.07.471485; this version posted December 9, 2021. The copyright holder for this preprint (which was not certified by peer review) is the author/funder, who has granted bioRxiv a license to display the preprint in perpetuity. It is made available under aCC-BY-NC-ND 4.0 International license.

differences in the population fractions in each cell cycle phase (see **Methods** and **Figure S2J**); even so, the differences in the dynamic responses were maintained (**Figure S2J**).

Our single cell data does also provide us an interesting perspective on whether NF-κB signaling dynamics can be considered oscillating or not, a topic that has been subjected to discussion (Barken et al., 2005; Kellogg and Tay, 2015; Nelson et al., 2004; Zambrano et al., 2016). Oscillations are characterized by the presence of multiple peaks in the NF-κB dynamic profiles. We calculated the fraction of cells with 1, 2 or 3 oscillatory peaks within each clonal population upon treatment with 10 ng/ml for 4 hours (**Figure 2D**) or longer (**Figure S2K**). We find that each clone contains a different fraction of cells that do not oscillate; however, there are also variable cell fractions in each clonal population that have two or more peaks and can be considered "oscillatory". The period of the oscillations, computed as inter-peak timing, is heterogenous but slightly higher for clone B (**Figure 2E**). Consistently with the dynamic heterogeneity found in each cell population, we find variability in the peak value ratios (**Figure 2F**) which is again maintained in experimental replicates (**Figure S2L**). Our data then show that being "oscillatory" is somehow a "fuzzy" phenotype and even clones derived from a population of quasi-identical cells can be considered oscillatory to different degrees. This compares with the qualitatively different dynamics observed for different cell types, that can go from cells that can oscillate in a sustained fashion for 20 hours and more (Kellogg and Tay, 2015) to those that oscillate in a more damped way with fewer oscillatory peaks (Zambrano et al., 2016) or do not oscillate at all (Lee et al., 2014).

Overall, our data shows how clonal populations of MEFs derived from the same mouse embryo have distinct dynamical features at population level both in their early response to TNF-α and in the subsequent dynamics, which is oscillatory to a different degree within each population. Yet, the dynamics is still considerably heterogeneous at single-cell level within each clonal population.

bioRxiv preprint doi: https://doi.org/10.1101/2021.12.07.471485; this version posted December 9, 2021. The copyright holder for this preprint (which was not certified by peer review) is the author/funder, who has granted bioRxiv a license to display the preprint in perpetuity. It is made available under aCC-BY-NC-ND 4.0 International license.

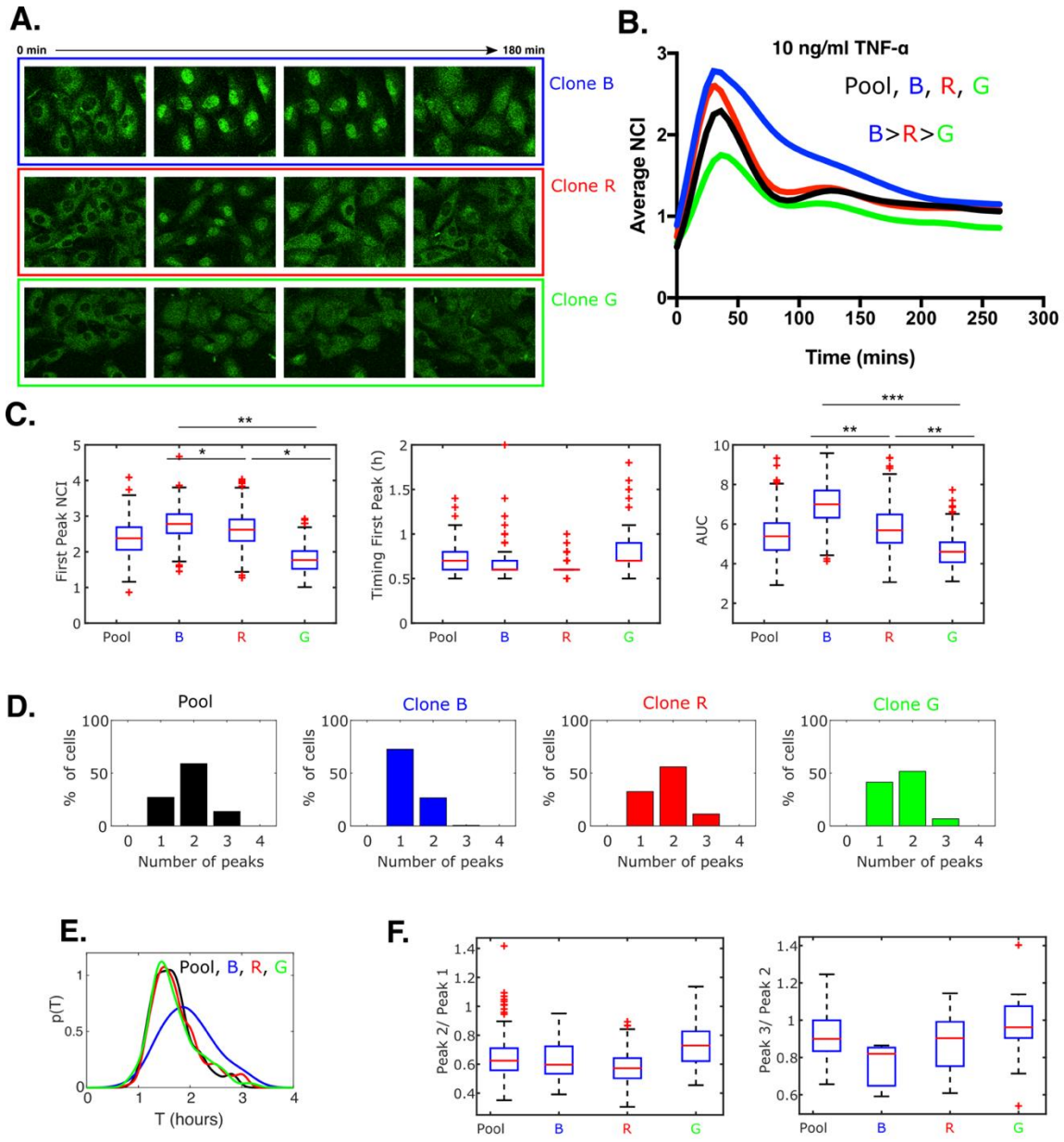

Figure 2. Clones B, R and G have distinct responses to TNF-α and are oscillatory to different degrees. **A.** Representative images from our time-lapse movies for clones B, R and G upon 10 ng/ml TNF-α stimulation. **B.** NF-κB dynamic response of the clones to TNF-α as assessed by the average NCI. **C.** The boxplots show the dynamical features of the response to TNF-α: NCI value of the first peak, timing of the first peak and area under the curve (AUC) in each population. **D.** Frequency of the number of the oscillatory peaks observed for each population in 4 hours. **E.** Periods of the oscillations computed as the inter-peak timing for each population. **F.** Ratios of the oscillatory peak values for each clonal population. In all panels *$p<10^{-2}$, ** $p<10^{-3}$, *** $p<10^{-4}$, multiple comparisons through Kruskal-Wallis.

bioRxiv preprint doi: https://doi.org/10.1101/2021.12.07.471485; this version posted December 9, 2021. The copyright holder for this preprint (which was not certified by peer review) is the author/funder, who has granted bioRxiv a license to display the preprint in perpetuity. It is made available under aCC-BY-NC-ND 4.0 International license.

3. Clonal populations have distinct transcriptional programs and control of target gene expression upon TNF-α

To further investigate to what extent our clonal populations are different, we next performed RNA-sequencing. Our clones display quantitative differences in their average NF-κB dynamic response already after 1 hour TNF-α stimulation (**Figure 2B**). Therefore, we performed RNA-sequencing after 1 hour (**Figure 3A**). To gain statistical power, we generated 5 replicates per condition (see **Methods**). All replicates were of good quality with more than 10000 genes with CPM>1 (see **Methods** and **Figure S3A**). An established reads mapping procedure (see **Methods**) confirms a frequency of single base substitution among clones compatible with the somatic mutation frequency (see **Figure S3B** and (Milholland et al., 2017)), as expected for cells derived from the same embryo.

We then performed a PCA of our samples' transcriptomes (see **Methods**) and found that samples from different clones do cluster in different groups (**Figure 3B**). Such neat clustering is also preserved in additional dimensions and few dimensions are required to explain most of the variability (**Figure S3C**). Of note, the apparent transcriptional divergence between our clones is small: when we performed our PCA including also public transcriptomic data from other tissues (see **Methods**), the samples from our populations cluster very closely together and far from the outgroup sample (**Figure S3D**). We then looked at genes differentially expressed between clones that were untreated, which are in principle the most informative from the point of view of the cell's identity. The categories enriched (see **Methods**) are related to morphogenesis of different organs/tissues: epithelium, renal system, and skeletal system, to cite a few (**Figure 3C**). This suggests that our clonal MEF populations conserve characteristics of the primary MEFs that were presumably already committed to different tissues or anatomical compartments.

We next decided to focus on how NF-κB controls gene expression in the three clonal populations. First, we focused on 462 genes that we previously established as differentially expressed upon TNF-α stimulation (Zambrano et al., 2016). Interestingly, using this gene set the PCA now clusters samples both by treatment and by the population of origin (see **Figure 3D** and **Methods**). This also applies when considering additional PCA dimensions, while again few dimensions are required to explain the global transcriptomic variability (**Figure S3E**).

We then had a closer look at the differentially expressed genes upon TNF-α in each clonal population through volcano plots (see **Figure 3E**, **Figure S3F** and **Methods**). Interestingly, the number of up-regulated genes correlates well with the strength of the NF-κB response and satisfies the same order relation B>R>G (**Figure 2B**). When performing gene set enrichment of up-regulated genes, the recurrent categories included TNF-α response and innate immune responses as expected (see **Methods** and **Figure S3G**), but with different degrees of overlap with the different categories, suggesting (along the lines of our PCA for NF-κB target genes) that the clones activate also slightly different transcriptional programs upon TNF-α.

Our results show that the clones differ mostly for developmental identity, and that they differentially express targets of NF-κB. The strength of the NF-κB response is a key determinant –but not the only one– of NF-κB target gene expression levels upon TNF-α stimulation.

bioRxiv preprint doi: https://doi.org/10.1101/2021.12.07.471485; this version posted December 9, 2021. The copyright holder for this preprint (which was not certified by peer review) is the author/funder, who has granted bioRxiv a license to display the preprint in perpetuity. It is made available under aCC-BY-NC-ND 4.0 International license.

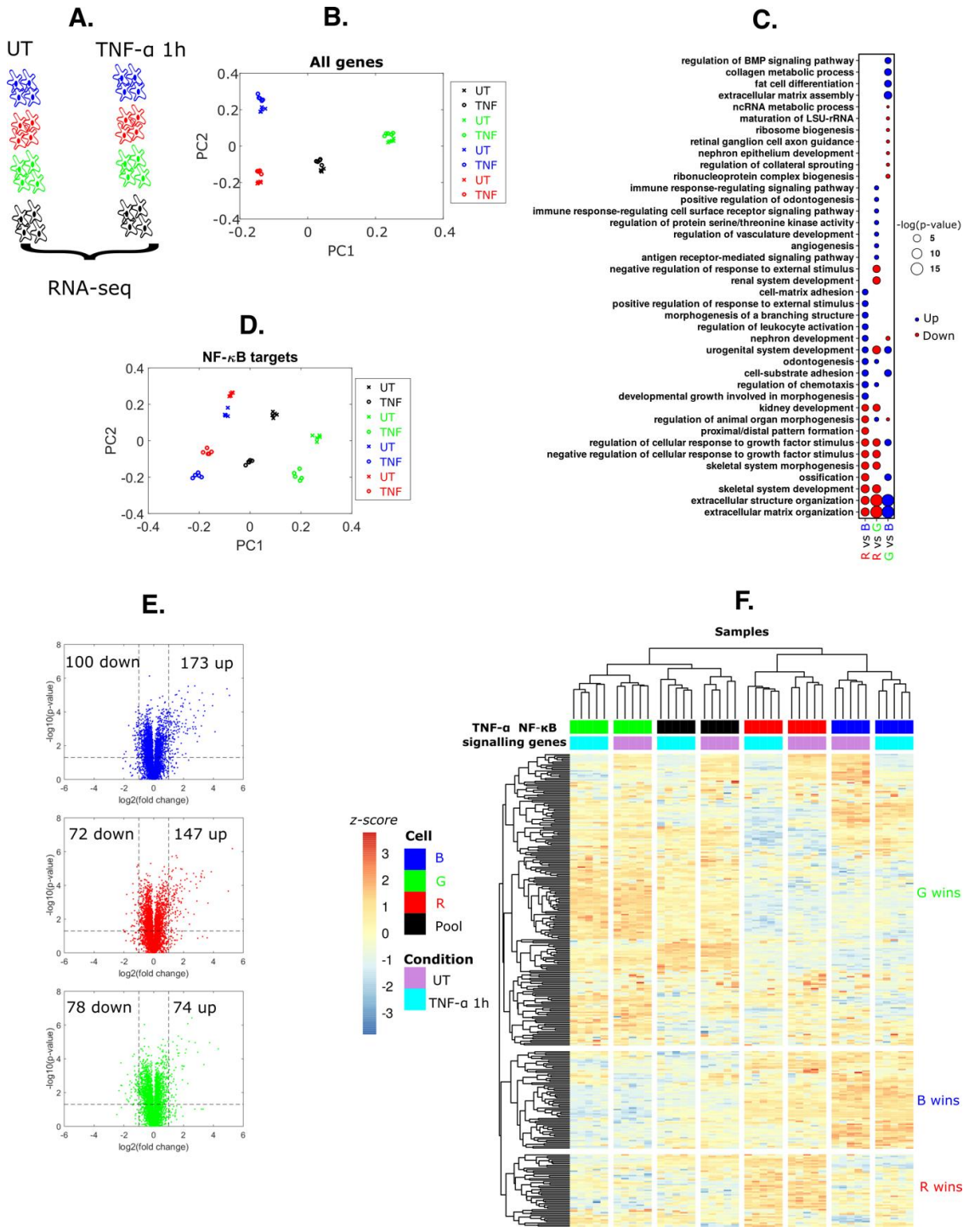

Figure 3. Clones B, R and G have distinct transcriptional programs. A. Scheme of the RNA-sequencing performed: cells treated 1 hour with 10 ng/ml TNF-α or untreated (UT). **B.** PCA of the UT and TNF-α samples of our clones B, R, G, and the pool, considering all genes. **C**. Gene ontology analysis of the differentially expressed genes between the clonal populations. **D.** PCA considering only NF-κB targets. **E.** Volcano plots of gene expression upon TNF-α for clone B, R and G (each dot is a single gene); p-values assessed through Student's t-test. **F.** Hierarchical clustering of the genes from the "TNF-α NF-κB signaling pathway (Mus musculus)" list from *Wikipathways*.

bioRxiv preprint doi: https://doi.org/10.1101/2021.12.07.471485; this version posted December 9, 2021. The copyright holder for this preprint (which was not certified by peer review) is the author/funder, who has granted bioRxiv a license to display the preprint in perpetuity. It is made available under aCC-BY-NC-ND 4.0 International license.

4. Differences in the transcriptional levels of proteins involved in NF-κB activation are predictive of the early response to inflammatory stimuli

Since the clearest phenotypic difference among our clonal populations is the different dynamic response to TNF-α we focused on the genes involved in NF-κB regulation (as opposed to genes that are NF-κB targets). The *wikipathways* database provides a list of hundreds of genes (see **Methods**) involved in TNF-α signaling. Of note, mutation calling did not highlight any differences in the mRNA sequences of these genes (see **Methods**). We then performed transcriptomic analysis on this group of genes (see **Methods**). The transcriptomic data cluster nicely across clones and treatments. Interestingly, unsupervised hierarchical clustering (**Figure 3F**) identifies three groups of genes: one more highly expressed in clone G, a second more highly expressed in clone B, and a third more highly expressed in clone R. The most common situation for any gene is to be more expressed in clone G (**Figure S3H**); this is not the case when we consider differentially expressed NF-κB targets, which are typically more highly expressed in clone B as expected from its strongest NF-κB dynamical response (**Figure S3I**).

The nuclear localization of NF-κB upon TNF-α is positively regulated by a variety of proteins including receptors, signal transducers and kinases (Hayden and Ghosh, 2008). We combined online databases (see **Methods**) and the literature (DeFelice et al., 2019; Hayden and Ghosh, 2008; Lee et al., 2016) to create a list (see **Figure 4A** and **Methods**) of the genes involved in NF-κB activation (a subset of the list from the *wikipathways* database) and we labeled it as "TNF-α to NF-κB". We hypothesized that the expression level of genes in the "TNF-α to NF-κB" list would positively affect the strength of NF-κB response in our clonal populations. Although the proportionality between transcript and protein amounts is not perfect nor constant (Schwanhäusser et al., 2011), for each gene we expect the proportionality to be very similar in each of our clonal populations. Indeed, the levels of expression of p65 (RelA) correlate well with the protein amount (computed as fluorescent signal intensity) across the clones (**Figure S4A**).

We focused on the basal expression levels of "TNF-α to NF-κB" genes in untreated samples. Their relative variation of the expression levels of these genes is moderate among clones, and only in exceptional cases goes beyond 0.5 or 1.5 times the average expression of each gene (**Figure 4A**). In our list, the average relative expression values of the list (see **Methods**) follow the order relation B>R>G. The absolute differences might seem small, so we evaluated the statistical probability of getting the B>R>G order relation with these differences of average relative expression or larger. We created 20000 random gene lists with the same size and similar expression levels (see **Methods** and **Figure S4B**) and found that the p-value of getting B>R>G order and size of differences is smaller than 0.005. We conclude that clone B has statistically significant highest basal expression of genes in the "TNF-α to NF-κB" list, which correlates with its strongest NF-κB response to TNF-α. Notably, this must be contrasted with our observation that in general clone G (rather than clone B) has more genes with higher expression values (**Figure 3F** and **S3H**).

Since this approach correctly predicted the correlation between strength of the response and expression levels of the genes involved in TNF-α signal transduction, we asked if it could also predict the relative clonal differences in the response to a different inflammatory stimulus. We focused on IL-1β, a cytokine that is known to activate NF-κB through a pathway only partially overlapping with that of TNF-α, and

bioRxiv preprint doi: https://doi.org/10.1101/2021.12.07.471485; this version posted December 9, 2021. The copyright holder for this preprint (which was not certified by peer review) is the author/funder, who has granted bioRxiv a license to display the preprint in perpetuity. It is made available under aCC-BY-NC-ND 4.0 International license.

characterized by its own regulatory mechanisms and dynamical features (DeFelice et al., 2019; Martin et al., 2020). We elaborated a list of "IL-1β to NF-κB" genes that are as well positive regulators of the NF-κB response upon IL-1β, including new genes such as *Ilr1r1,* the gene encoding the IL-1β receptor, and *MyD88* (**Figure 4B**). In this list, we found again different levels of expression that typically do not exceed 2-fold (**Figure 4B**). Interestingly, in this case the order relation of the average expression was different: B>G>R. By reproducing the bootstrapping analysis used before, we find that the order relation B>G>R and the size of the differences are infrequent in random gene lists with similar features, with p<0.015 (see **Methods** and **Figure S4C**). We then performed live cell imaging of the clones upon 100 ng/ml IL-1β. All clones respond, and in particular now G has a stronger response to IL-1β than to TNF-α (**Movies S5** and **S6** and **Figure 4C**); notably, the average NF-κB response reflects the order relation B>G>R (**Figure 4D**), as predicted. Differences are also clear when considering single-cell data (**Figure 4E**, **S4D**), where we can see now that clone G cells display overall a stronger response than clone R cells. However, clone B is the one with a higher response and a much higher AUC. Finally, upon IL-1β we find that the cells' oscillatory phenotype is different relative to TNF-α: more cells of clone G have at least two peaks (**Figure 4F**) and an oscillatory period at T=1.5h, similar to clone R (**Figure 4G**). Clone B remains the one with a less oscillatory phenotype (**Figure 4F**), suggesting that this behavior might be related with downstream regulators of NF-κB activity, an idea that we explore next. As with TNF-α, oscillations are also heterogeneous across the clones (**Figure S4E**).

Taken together, our data shows that the expression levels of genes coding for proteins in two different signaling cascades upstream of NF-κB predict which cells respond more or less intensely to which inflammatory stimulus.

bioRxiv preprint doi: https://doi.org/10.1101/2021.12.07.471485; this version posted December 9, 2021. The copyright holder for this preprint (which was not certified by peer review) is the author/funder, who has granted bioRxiv a license to display the preprint in perpetuity. It is made available under aCC-BY-NC-ND 4.0 International license.

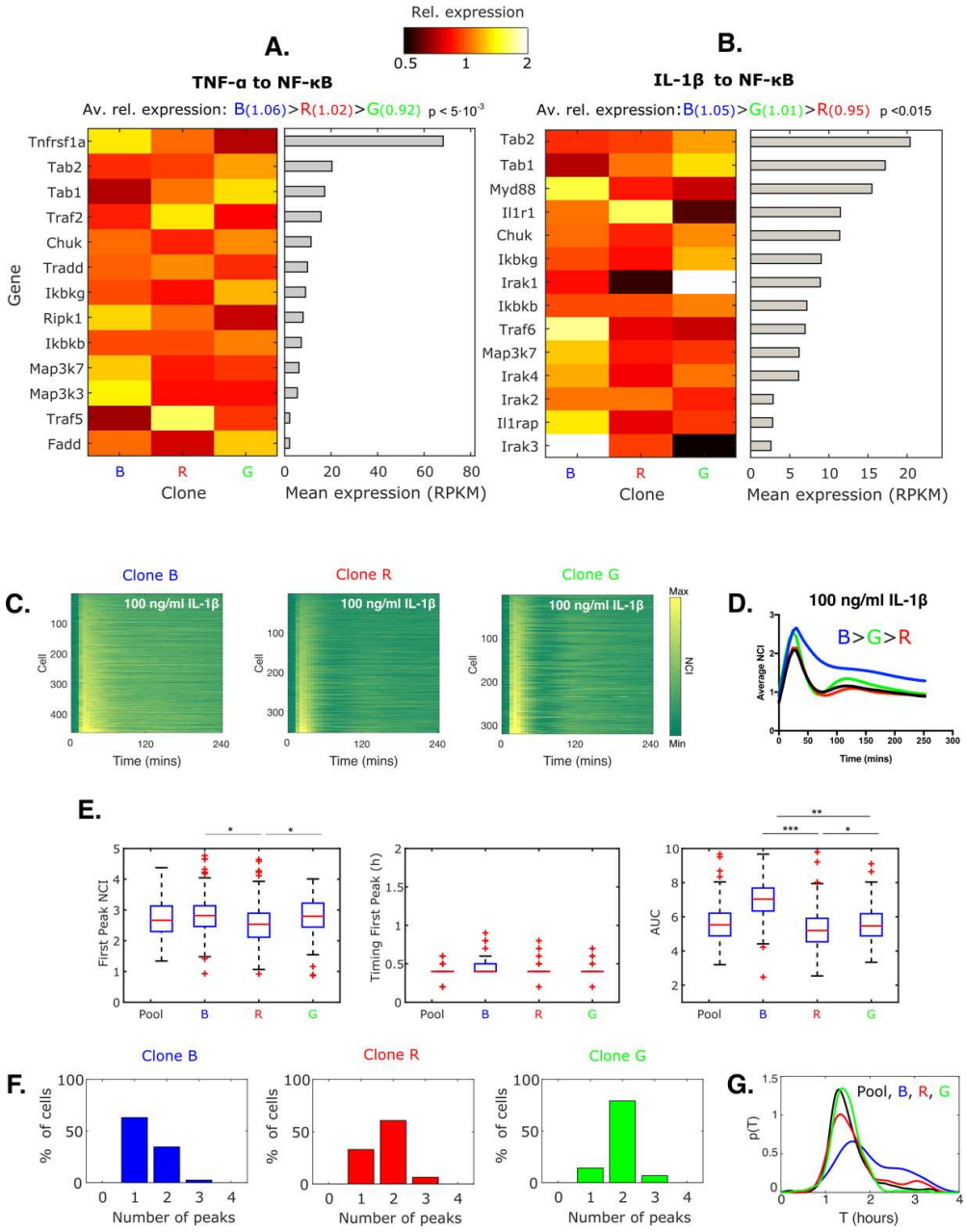

Figure 4. Differences in expression of genes involved in NF-κB activation correlate with NF-κB response to TNF-α and IL-1β. A. Relative expression levels (normalized in each gene by the average expression across clones) of genes of the "TNF-α to NF-κB" list encoding for proteins involved in NF-κB activation upon TNF-α (left) and average expression levels for each gene (right). The average relative expression of each clonal population and their order relation is shown on top. **B.** Same as in A but for genes of the "IL-1β to NF-κB" list, coding for proteins involved in NF-κB activation upon IL-1β. **C.** Dynamic heatmap of the responses of clone B, R and G to 100 ng/ml IL-1β. **D.** Average NF-κB response for the three clones upon IL-1β stimulation. **E.** The boxplots show the dynamical features of the response to IL-1β: value of the first peak, timing, and area under the curve (AUC). **F.** Fraction of the cells having 1, 2 or 3 oscillatory peaks on each of the populations considered upon IL-1β. **G.** Periods of the oscillations computed as the inter-peak timing for each population. *p<10^{-2}, ** p<10^{-3}, *** p<10^{-4}, multiple comparisons through Kruskal-Wallis.

bioRxiv preprint doi: https://doi.org/10.1101/2021.12.07.471485; this version posted December 9, 2021. The copyright holder for this preprint (which was not certified by peer review) is the author/funder, who has granted bioRxiv a license to display the preprint in perpetuity. It is made available under aCC-BY-NC-ND 4.0 International license.

5. Differences in the expression levels of the negative feedbacks underpin distinct NF-κB dynamics in quasi-identical cells

Beyond differences within the first 30 minutes, our clonal populations also show differences at later time points, with clone R having a sharper NF-κB response as compared to clone B, i.e. its NF-κB nuclear localization decays faster (Zambrano et al., 2020). We investigated if transcriptomic data could also shed light on the origin of these differences. It is well established that NF-κB nuclear localization dynamics is tightly regulated by a system of negative feedbacks such as the inhibitors IκBα, IκBβ and IκBε that keep NF-κB in the cytosol (A.Hoffmann et al., 2002; Paszek et al., 2010) and the protein A20 that interferes with stimulus-mediated IκB degradation (Ashall et al., 2009; Son et al., 2021); all of them are under the transcriptional control of NF-κB (**Figure 5A**). We then elaborated a list of "NF-κB negative feedbacks". They are all expressed upon TNF-α activation after 1 hour (**Figure 5B**); these are genes that respond relatively quickly, as we could observe previously (Zambrano et al., 2016) (**Figure S5B**). Indeed, we found differences in the expression levels of "NF-κB negative feedbacks" genes across the clones, albeit moderate (**Figure 5B**). Average relative expression levels are in the order R>B>G with numerical values leading to $p<0.002$ (see **Methods** and **Figure S5A**). This correlates with a sharpest response of the clone R as compared to clone B (the expression levels of the negative feedbacks are lower for clone G, which is the least responding one). Indeed, the expression levels for IκBα (*Nfkbia*) and IκBε (*Nfkbie*) are higher in clone R with respect to clone B (**Figure S5C**). RT-qPCR also confirms mRNA levels of negative feedbacks differ between clones (**Figure S5D**).

The negative feedback loops of the NF-κB system have been extensively modelled (A.Hoffmann et al., 2002; Nelson et al., 2004; Paszek et al., 2010) and thus mathematical modelling could provide us further insights on whether transcriptional differences in the "NF-κB negative feedbacks" are enough to explain the differences observed in the sharpness of the NF-κB response (details provided in **Methods**). Thus, we built a new extended mathematical model that includes IκBβ and IκBε in addition to IκBα and A20 feedbacks present in our previous model (Zambrano et al., 2016) (see **Methods**). The new model contains our original set of parameters (Zambrano et al., 2016) and the selection of new parameters for the additional feedbacks is constrained in such a way as to reproduce the relative expression levels of the feedbacks in clone R (see **Methods**). We took the clone R parameter set and modified it (see **Methods**) to obtain a new parameter set for clone B, so that the relation between the expression of the inhibitors between both clones are preserved (see **Methods**). We also varied the levels of NF-κB according to the experimentally observed levels of expression (**Figure S4A** and **Methods**). Interestingly, these small differences already lead to a change in the dynamics from sharp in the simulation of R to persistent in that of B, qualitatively similar to the one observed experimentally (**Figure 5C**).

Since our modelling result could be due to our particular selection of parameters, we performed simulations for randomly generated parameter sets (see **Figure 5D** and **Methods**). Random parameter sets for clone R and clone B are generated so they satisfy the constraints described in the previous paragraph (the ratios of the relative expression of the inhibitors within and between the clones match the experimentally observed ones in the resulting simulations **Figures 5E** and **5F**). In doing so, for most of the random parameter sets we recapitulate our experimental observations: moderate differences in the

bioRxiv preprint doi: https://doi.org/10.1101/2021.12.07.471485; this version posted December 9, 2021. The copyright holder for this preprint (which was not certified by peer review) is the author/funder, who has granted bioRxiv a license to display the preprint in perpetuity. It is made available under aCC-BY-NC-ND 4.0 International license.

timing and the first peak of the response (**Figure 5G**), whereas there is a more drastic decrease of the sharpness for clone B, as revealed by the AUC (**Figure 5G**). This mirrors the sharper NF-κB nuclear localization dynamics that we found experimentally for clone R relative to B (see e.g., **Figure 2C**). Thus, mathematical modelling shows how the moderate transcriptional differences observed, combined, can have a clear impact in the dynamics and might be the key driver of the differences observed.

To confirm the role of small transcriptional differences on the dynamics emerging from our bioinformatic and modelling analysis, we set out to experimentally test the effect of modulating the NF-κB repressor levels in the dynamic response to TNF-α. We focused on the key inhibitor IκBα, whose absence gives rise to a non-oscillatory phenotype (A.Hoffmann et al., 2002; Cheng et al., 2021). To modulate the mRNA levels of IκBα we took advantage of antisense oligonucleotide (ASO) technology (see **Methods**). The single-stranded synthetic nucleic acid analogs (2'-deoxy-2'-fluoro-β-d-arabino nucleic acid, FANA) were designed to be self-delivered to the cells and to be fully complementary to the mRNA of interest. They induce mRNA cleavage by RNAseH to reduce the synthesis of the encoded protein (see **Methods** and **Figure 5A**). We pre-treated for 24 hours clones R and B with different concentrations of the ASO, whose internalization was visible (**Figure S5E**), and this led to a moderate but significant decrease on the mRNA levels of IκBα (**Figure S5F**). We indeed observed that, upon TNF-α, the response of both clone B (**Figure 5H**, top panels) and clone R (**Figure 5H**, bottom panels) was characterized by a more persistent NF-κB nuclear localization, indicating that partial transcriptional disruption of the IκBα negative feedback is enough to produce a qualitative change in the dynamics (**Movies S7** and **S8**). This was also the case when pre-treating our MEFs pool with ASOs (**Figure S5G**). A more detailed quantification of the dynamics shows that the maximum value of the NF-κB response does not change much in ASO-treated cells (**Figure 5I**). However, the area under the curve upon TNF-α increases for both clones, and in particular for clone R, so that the AUC of clone R is much more similar to that of clone B. This trend is reproducible in replicates (**Figures S5H, S5I**).

Overall, we have shown how the expression levels of the negative feedbacks correlate with the differences of NF-κB dynamics observed across our clones, and especially with the observed sharp versus persistent NF-κB response. Our experiment-driven simulations also indicate that NF-κB negative feedbacks are key determinants of the distinct dynamics observed in our clonal populations. Finally, our experiments with ASOs show how even a mild targeted modulation of the expression of IκBα can distinctly alter the dynamics of clone R to resemble that of clone B, and therefore to reprogram it from a sharp (and oscillatory) NF-κB activation to a persistent response.

bioRxiv preprint doi: https://doi.org/10.1101/2021.12.07.471485; this version posted December 9, 2021. The copyright holder for this preprint (which was not certified by peer review) is the author/funder, who has granted bioRxiv a license to display the preprint in perpetuity. It is made available under aCC-BY-NC-ND 4.0 International license.

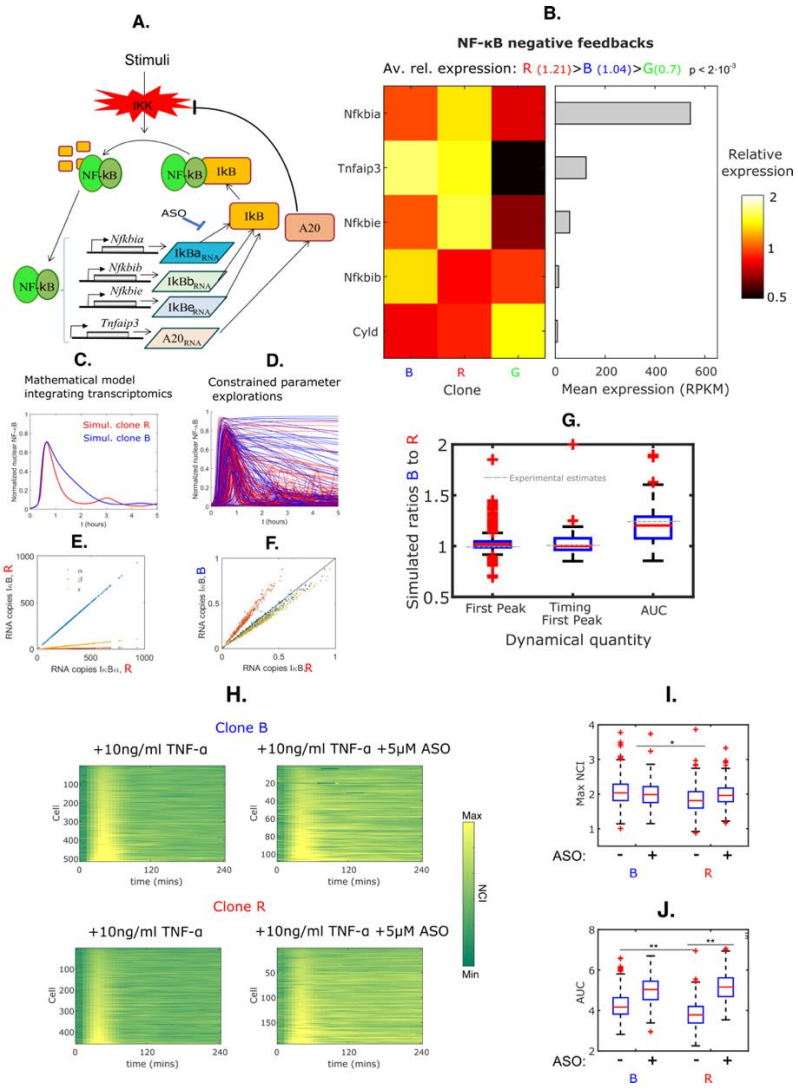

Figure 5. Differences in expression levels of NF-κB negative feedbacks can reproduce the observed dynamical differences between clones. A. Scheme of the NF-κB genetic circuit with main negative feedback regulators. **B.** (Left) Relative expression levels (normalized by the average expression across clonal populations) of genes of the "NF-κB negative feedbacks" list upon TNF-α and (right) average expression levels for each gene. The list includes those in panel A. The order relation of the average relative expression levels is shown on top. **C.** Transcriptionally constrained numerical simulation of clone R (red line) and clone B (blue line). **D.** Example of numerical simulations of randomly generated parameters of clone B and clone R where the experimental ratios of expression of the transcripts are kept constant and equal to those experimentally observed. **E.** The ratios between the levels of expression of the inhibitors within the simulated clone R are preserved and **F.** the ratios between values observed in clone B and clone R are preserved too. Each dot corresponds to simulations of a parameter set randomly generated and satisfying our constraints. **G.** Ratios between values observed for constrained simulations of clone B and clone R for the timing and value of the first peak and area under the curve. **H.** Representative dynamic heatmaps of clone B (top) and clone R (bottom) upon TNF-α for both untreated and ASO-treated cells. **I.** Quantification of the maximum response for untreated and ASO-treated cells upon TNF-α. **J.** Quantification of the AUC for untreated and ASO-treated cells upon TNF-α, *$p<10^{-2}$, ** $p<10^{-3}$, *** $p<10^{-4}$, multiple comparisons through Kruskal-Wallis.

bioRxiv preprint doi: https://doi.org/10.1101/2021.12.07.471485; this version posted December 9, 2021. The copyright holder for this preprint (which was not certified by peer review) is the author/funder, who has granted bioRxiv a license to display the preprint in perpetuity. It is made available under aCC-BY-NC-ND 4.0 International license.

DISCUSSION

A population of MEFs with heterogeneous NF-κB dynamics is composed by sub-populations of quasi-identical cells with distinct dynamics. Single-cell imaging studies of NF-κB dynamics have shown that there is a high degree of heterogeneity within cell populations (Lee et al., 2014; Nelson et al., 2004; Paszek et al., 2010; Sung et al., 2009; Tay et al., 2010; Zhang et al., 2017a). Our work, performed on a very homogenous cell population of mouse embryonic fibroblasts immortalized by serial passages and derived from a single embryo, indicates that NF-κB dynamic heterogeneity might be due in part to the coexistence of subpopulations of quasi-identical cells that do respond distinctly to the stimuli. Extrinsic factors such as the cell cycle phase have been shown to affect NF-κB dynamics (Ankers et al., 2016) but we cannot attribute inter-clonal differences to differences in the cell cycle. Instead, we show here that the expression levels of genes coding for elements of the NF-κB regulatory circuit can explain the clonal differences, suggesting that they are a key determinant of the dynamical heterogeneity observed in the original population.

Transcriptomics is predictive of the clonal response to stimuli. The link between NF-κB dynamics and transcription is typically analyzed in one direction: how does NF-κB nuclear localization dynamics drive gene expression? (Lane et al., 2017; Lee et al., 2014; Tay et al., 2010; Zambrano et al., 2016). Here we consider the same question in the other direction: how can transcriptomic differences affect dynamics? We developed a computational framework based on the average expression levels of key genes coding for regulatory elements upstream of NF-κB, which explains differences in the strength of the response of clones to TNF-α. The same framework predicts clonal differences in the response to IL-1β. The expression level of these genes coding for upstream positive regulators could indeed determine the amount of IKK complex formed upon both stimuli, which has been recently shown to correlate with NF-κB activation (Cruz et al., 2021). We also show here how the expression levels of the components of the negative feedback of NF-κB predict whether the NF-κB response will be sharp or persistent. The prediction is supported by mathematical modelling and experimental data showing that a moderate reduction in IκBα level induced by antisense oligonucleotides can lead to relatively large differences in the NF-κB dynamics. Knock-out of IκBα gene *Nfkbia* has been shown to induce a change from oscillatory to sustained dynamics (Cheng et al., 2021), our work shows how a finer tuning of the feedback expression can produce analogous changes in NF-κB dynamics.

Part of the success of our approach is probably due to the biological homogeneity of the clones, which derive from cells of the same type that come from a single embryo. We assume that transcriptional levels are informative of protein levels; while this is not necessarily true, every deviation from the assumption will be identical in each clone. We hypothesize that a similar transcriptional approach could be used to predict the relative difference in the dynamic response of other TFs in subpopulations within other relatively homogeneous cell populations, as for example in cells derived from the same tissue or in clones within a tumor mass (Greaves and Maley, 2012) that might respond differently to therapy (Paek et al., 2016).

NF-κB oscillatory phenotype is fuzzy. NF-κB nuclear localization dynamics in single living cells was observed for the first time more than 15 years ago (Nelson et al., 2004) and since then its oscillatory

bioRxiv preprint doi: https://doi.org/10.1101/2021.12.07.471485; this version posted December 9, 2021. The copyright holder for this preprint (which was not certified by peer review) is the author/funder, who has granted bioRxiv a license to display the preprint in perpetuity. It is made available under aCC-BY-NC-ND 4.0 International license.

nature was subject to discussion (Barken et al., 2005; Nelson et al., 2005). More recently, we argued that NF-κB displays damped oscillations (Zambrano et al., 2016) as compared to the sustained oscillations reported by others (Kellogg and Tay, 2015). Our present work shows that classification of NF-κB dynamics is not necessarily binary. Within a population of quasi-identical cells, we can find sub-populations of cells that are more and less prone to oscillate. For circadian oscillators as well it was found that clonal populations have different oscillatory features (Li et al., 2020). For our cells, we show that this largely depends on the expression level of genes belonging to the NF-κB regulatory circuit. We previously proposed that oscillations are a way to provide opportunity windows for decision (Zambrano et al., 2016), and this work shows such windows can be diverse across cell subpopulations, which can contribute to population robustness in response to stimuli (Paszek et al., 2010). On the other hand, our work sheds light on the origin of the dynamic variability reported in the literature: if small transcriptional differences can affect the dynamics of NF-κB, it is not surprising that different cell types have completely different oscillatory phenotypes.

Stimulus specificity in the NF-κB response is clone-dependent. The increasing availability of single-cell data on NF-κB dynamics has shown that it is possible for cells to discriminate between stimulus type (Adelaja et al., 2021; Cheng et al., 2021; Martin et al., 2020), dose (Tay et al., 2010; Zambrano et al., 2014a; Zhang et al., 2017a) and dynamic profile (Ashall et al., 2009; Lee et al., 2016; Zambrano et al., 2016). Here, we find that two MEF clones from the same embryo, clone G and clone B, do respond differently to two different stimuli: clone G responds strongly to IL-1β, while clone B responds strongly to both TNF-α and IL-1β. On the other hand, clone R produces a sharper and more oscillatory NF-κB response than clone B. This indicates that stimulus specificity in NF-κB dynamics is clone-dependent and, all the more so, that it will vary among cell types within the same organism. A recent study shows that a synthetic version of the NF-κB circuit ectopically expressed in yeast (Zhang et al., 2017b) displays different types of dynamics and responses by manipulation of the key kinetic parameters. Furthermore, since immortalized MEFs maintain certain characteristics of primary MEFs (Beg and Baltimore, 1996; Gapuzan et al., 2005), our work suggests that a similar fine-tuning can take place naturally in primary mammalian cells.

Origin of the transcriptional differences across clones. We show that the dynamical differences observed between clones are robust and persist over time and cell culturing. Persistent transcriptional differences can be due to sequence variants in the control elements of the genes, especially in enhancers (Natoli and Ostuni, 2019), or in epigenetic changes in DNA methylation or chromatin accessibility of the same control elements. Our RNA-sequence based bioinformatic analysis did not detect any variant among clones in the mRNA sequence of genes involved in the NF-κB response. We inferred from it a substitution rate in the genome of the clones in the order of $5 \cdot 10^{-7}$ per base pair, which would translate to <100 substitutions per haploid genome. This substitution rate is consistent with somatic variability of cells from the same organism (Amand et al., 2016; Milholland et al., 2017). However, our analysis cannot detect other genetic changes, such as sequence changes in the regulatory regions or copy number variations. This genetic variability could contribute to the small (although robust) differences in gene expression reported here. The other possibility is epigenomic variation between different cells. We find that the most visible difference in the transcriptomics of the different clonal populations is related to developmental programs, which indeed involve epigenetic variations. Whether expression of different developmental programs

bioRxiv preprint doi: https://doi.org/10.1101/2021.12.07.471485; this version posted December 9, 2021. The copyright holder for this preprint (which was not certified by peer review) is the author/funder, who has granted bioRxiv a license to display the preprint in perpetuity. It is made available under aCC-BY-NC-ND 4.0 International license.

within different cells of the same population can give rise to the difference in response dynamics of NF-κB and other TFs remains to be proved, but we speculate that this is at least likely.

Cell to cell differences within clones. We find that the NF-κB dynamic response of the cells within each clonal population is still heterogeneous. We speculate that this cell-to-cell variability can have a purely stochastic component related to the probabilistic nature of the activation of gene transcription. Indeed, we recently found experimentally that even highly transcribed genes under the control of NF-κB like the one encoding for IκBα are transcribed stochastically (Zambrano et al., 2020). Thus, the same cell might be oscillatory or not at different times, depending on how recently it had a burst of IκBα transcription and translation. Future studies will be needed to connect the transcriptional history of each single cell with its NF-κB dynamics.

In sum, our work shows that part of the NF-κB dynamic heterogeneity observed within a relatively homogenous population of cells can be due to the co-existence of cell subpopulations with distinct dynamics, which correlates with robust although small differences in the expression levels of genes belonging to the regulatory circuit. However, some heterogeneity remains between cells of the same clone, suggesting that ephemeral variations of transcript levels follow transcriptional bursts in individual cells. We speculate that analogous mechanisms might also diversify the dynamic response of other TFs to external cues.

ACKNOWLEDGEMENTS

We acknowledge Prof. Manolis Pasparakis for sharing with us the immortalized MEF population from a single embryo, Prof. Roberto Sitia for suggesting the initial experiment and Davide Mazza and Nacho Molina for critical revision of the manuscript. We received funding from Ospedale San Raffaele (OSR Seed Grant to S.Z.), San Raffaele University (predoctoral fellowship to C.K.) and Associazione Italiana Ricerca sul Cancro (AIRC 2017-ID.18687, project PI A.A). Part of the present work was performed by CK in partial fulfillment of the requirements for obtaining the PhD degree at Vita-Salute San Raffaele University, Milano, Italy.

AUTHOR CONTRIBUTION

Conceptualization: SZ. Supervision: SZ, MEB, AA. Visualization: SZ, CK, EM, MEB. Formal Analysis: CK, SZ, EM, AA. Investigation: CK, SZ, EM, JGM, FB. Writing-Original draft: SZ, CK, MEB. Writing-review and Editing: SZ, CK, EM, MEB, AA, JGM, FB. Funding acquisition: SZ, MEB, AA.

DECLARATION OF INTERESTS

The authors declare no competing interests.

bioRxiv preprint doi: https://doi.org/10.1101/2021.12.07.471485; this version posted December 9, 2021. The copyright holder for this preprint (which was not certified by peer review) is the author/funder, who has granted bioRxiv a license to display the preprint in perpetuity. It is made available under aCC-BY-NC-ND 4.0 International license.

METHODS

Cell line and cell culture. GFP-p65 knock-in mouse embryonic fibroblasts (MEFs) were kindly provided by M.Pasparakis. MEFs were derived from a single embryo of homozygous knock-in GFP-p65 expressing mouse using standard protocols (De Lorenzi et al., 2009) and immortalized by serial passaging also known as the 3T3 method and typically involves 20-30 passages (Amand et al., 2016). The cells were cultured in phenol-red free DMEM supplemented with 10% FCS, 50 mM b-mercaptoethanol, 1x L-glutamine, 1x pen/strep, 1x sodium pyruvate and 1x non-essential amino acids. MEFs were subcultured every 2-3 days before they reached 100% confluency and kept at 37°C and 5% CO2.

Generation of the clonal populations by single cell cloning. MEFs were harvested by 1x Trypsin solution and counted. Final concentration of 5 cells/ml was achieved by serial dilutions and 100 µl of the cell suspension per well were pipetted to a 96-well plate. The plate was screened for single colonies and selected colonies were then expanded.

Cell treatments. Where indicated the cells were stimulated with the final concentration of 10 ng/ml of recombinant human TNF-α protein (R&D Systems) or 100ng/ml of recombinant human interleukin 1 beta (IL-1β, PeproTech).

Live cell imaging. Live cell imaging of GFP-p65 knock-in MEFs was performed as in (Zambrano et al., 2016). We used a Leica TCS SP5 confocal microscope with an incubation system where cells were stably maintained at 37°C in 5% CO2. Time-lapse images were acquired at 6 min intervals for up to 10 hr. We used a low magnification objective (20x, 0.5 NA) and an open pinhole (Airy 3), ensuring that the image depth (10.7 µm) contains the thickness of the whole cell so that images capture the total cell fluorescence. GFP-p65 is imaged with the 488 nm Argon laser (GFP channel) while Hoechst 33342 stained nuclei are imaged with the low energy 405 nm UV diode laser at 5% of its maximum intensity (HOE channel). The staining was performed at room temperature for 10-15 minutes using NucBlue™ Live ReadyProbes™ Reagent, ThermoFischer), 1:100 v/v and incubated 10-15 min at RT, which we showed previously does not interfere with the response to TNF-α (Zambrano et al., 2016). Images were acquired as 16 bit, 1024×1024, TIFF files. Experiment replicates were performed on different days. In each experiment we typically imaged more than one clone in different wells of an 8-well labtek.

Automated quantification of NF-κB dynamics in single living cells. To quantify NF-κB nuclear localization dynamics in living cells, we follow our previously described procedure of normalizing the average nuclear signal intensity by the average cytosolic fluorescence intensity (Zambrano et al., 2016) to obtain the nuclear to cytosolic intensity (NCI), also used by others (Kellogg and Tay, 2015; Paszek et al., 2010). We improved our custom-made routines that run on MATLAB R2015 and are available upon request. In short, nuclei are segmented based on the intensity of the HOE channel, and nuclear masks are used to compute the nuclear average NF-κB intensity in each cell. In order to estimate the average cytoplasmic NF-κB intensity, first the background was computed by taking a square area centered on the cell nucleus, dividing it in tiles and using the one with the smallest average intensity in the GFP channel. After this, pixels belonging to the cytoplasm are those with intensity above the background on a ring around each nucleus

bioRxiv preprint doi: https://doi.org/10.1101/2021.12.07.471485; this version posted December 9, 2021. The copyright holder for this preprint (which was not certified by peer review) is the author/funder, who has granted bioRxiv a license to display the preprint in perpetuity. It is made available under aCC-BY-NC-ND 4.0 International license.

of width 0.5 times the nuclear radius. Tracking of cells between frames is performed through an optimized algorithm based on the Hungarian linker method (Careccia, 2019). Cells are discarded upon abrupt changes of the nuclear and/or cytosolic areas, indicative of erroneous tracking or cell death or mitosis.

Stochastic clustering of the* NF-κB *dynamic profiles. We performed an unsupervised clustering of NF-κB dynamic profiles from cells of the 8 clones using the k-means algorithm (k=8) based on the Euclidean distance between profiles (MATLAB). In each realization we randomly picked 50 profiles from each clonal population. The profiles are clustered then in 8 groups (**Figure S1B**), and we compute the number of cells from each clonal population in each cluster (**Figure S1C**). In each realization we compute p_{ik} , representing the fraction of trajectories of clone *k* that are present in the cluster where the clone *i* has a higher number of clustered profiles. For *k=i*, it represents the fraction of cells of the clone *i* in the cluster where it is more represented. The result for a single realization is shown in **Figure S1D**. For each realization we computed the disorder parameter defined as $S = -\sum_{i,j} p_{ij} \log p_{ij}$ and compared with the same result when the dynamic profiles are randomly assigned to the eight clonal populations and then clustered stochastically. We followed this procedure 500 times and the disorder parameter was always higher for cells randomly assigned to clonal populations, indicating further that NF-κB dynamic profiles are clustered according to a certain pattern strongly related with the clonal population of origin.

Analysis of NF-κB dynamics. To extract the dynamic features of the NCI time series we followed the same procedure as in (Zambrano et al., 2014a, 2016). In short, NCI series are smoothed, and peaks are detected using standard MATLAB functions (*smooth* and *pkfnd*, respectively) and those with a prominence θ>0.15 are considered real peaks. This value is well beyond the prominence of noisy peaks found in this type of datasets (Zambrano et al., 2016) and provides a reasonably good compromise between the need to ignore noise peaks and the need to detect small peaks of valuable dynamical information (e.g. if a cell is oscillating or not). The timing of the peak was determined considering the maximum value. Instead, the area under the curve is calculated as the integral in the time interval considered of NCI(t).

Cell cycle analysis. Cell cycle analysis was done as described in (Brambilla et al., 2020): MEFs were harvested and fixed with cold 70% ethanol and kept overnight at -20°C. Cells were then washed once with 5% FBS/PBS and stained with PBS containing 10 µg/ml propidium iodide and 10 µg/ml RNAse A for 1 hour at room temperature. Samples were then read at a cytometer using a 488 nm laser.

Cell cycle computational correction: An artificial dataset of NCI time series of clone R were generated: the top 25% of the population was assumed to be the S-phase high responders (Ankers et al., 2016) and their percentage was increased to 43% by neglecting the corresponding fraction of the less responding cells. The resulting dataset has a higher value than the original but still a lower value of the AUC than clone B (**Figure S2J**) which makes it unlikely that cell cycle is the key driver of this inter-clonal difference, as for the differences between B and G detailed in the text.

bioRxiv preprint doi: https://doi.org/10.1101/2021.12.07.471485; this version posted December 9, 2021. The copyright holder for this preprint (which was not certified by peer review) is the author/funder, who has granted bioRxiv a license to display the preprint in perpetuity. It is made available under aCC-BY-NC-ND 4.0 International license.

RNA isolation and real time PCR. 1.5x10^5 MEFs were plated on a 6-well plate a day before the extraction. Total RNA was isolated using the NucleoSpin RNA II kit (Macherey-Nagel). The amount of RNA was determined using a NanoDrop spectrophotometer (Thermo Fisher Scientific) and 1 μg was then reverse transcribed using SuperScript IV Reverse Transcriptase (Thermo Fisher Scientific). qPCR was performed using LightCycler 480 SYBR Green I Master (Roche). The expression of *IκBa* and A20 were checked using following primers:
IκBa forward: 5' CTTGGCTGTGATCACCAACCAG 3'
IκBa reverse: 5' CGAAACCAGGTCAGGATTCTGC 3'
A20 forward: 5' ACAGAGCAGGGACAAGCAAGTG 3'
A20 reverse: 5' GTTTAGGGGGCTCTTCAGGC 3'

RNA sequencing and Bioinformatic analysis. Libraries for Illumina NGS were prepared as described in (Brambilla et al., 2020). After trimming the adapter sequences (cutadapt, https://cutadapt.readthedocs.io) reads were mapped to mouse genome (mm10) using hisat2 (http://daehwankimlab.github.io/hisat2/) using parameters "-p 20 -5 5".
Read counting was performed using featureCounts from the Subread Package and features displaying less than 10 reads were filtered out. Differential expression analysis was performed using DESeq2 (https://bioconductor.org/packages/release/bioc/html/DESeq2.html) with the following design formula "=~ 1 + clone + treatment + clone:treatment".
Principal component analysis (PCA) was performed using MATLAB, keeping only genes for which RPKM>1 in at least five samples. Additional RNA-seq samples from several mouse tissues were retrieved from the ENCODE Database (https://www.encodeproject.org). Volcano plots were generated using MATLAB and p-values derived from the t-test statistics. Gene ontology was performed using the "*clusterProfiler*" R package (https://bioconductor.org/packages/release/bioc/html/clusterProfiler.html). Heatmap and Hierarchical clustering was performed using the "*Pheatmap*" R package.
Genes annotated in the mouse TNF-signalling were retrieved from WikiPathway (https://www.wikipathways.org/index.php/Pathway:WP246)

Estimation of the genetic differences between clonal populations. The SNP calling step was performed using the GATK 3.6 toolkit (McKenna et al., 2010) in order to split splice junction reads, to recalibrate quality scores and to call variants. To minimize false positive variants the GATK Variant filtration tool was used using the following parameters:
"--filterExpression QD < 5.0 --filterExpression DP < 10 --filterExpression ReadPosRankSum < -8.0 --filterExpression MQRankSum < -12.5 --filterExpression MQ < 40.0 --filterExpression FS > 60.0". Nucleotide positions with heterozygosity scores < 0.10 were excluded as previously described (Adetunji et al., 2019). We called SNPs with different levels of confidence based on three different coverage cut-offs (5x, 10x, 20x) and then we calculated the number of unique SNPs for each clone. We find that our clones differ in a range of 200-400 nucleotides (**Figure S3B**, **Table S2**) which, once divided by the length of the genome at the specific coverage cut-off, provided us a "mutation rate" of approximately 5·10-7 per base pair (**Figure S3B**). Interestingly, this is of the order of magnitude of the somatic mutation rate found between somatic cells from the same mouse (Milholland et al., 2017) indicating how the frequency of SNPs for our clones correspond to "somatic differences" that can be found between cells of the same organism. Of note, our

bioRxiv preprint doi: https://doi.org/10.1101/2021.12.07.471485; this version posted December 9, 2021. The copyright holder for this preprint (which was not certified by peer review) is the author/funder, who has granted bioRxiv a license to display the preprint in perpetuity. It is made available under aCC-BY-NC-ND 4.0 International license.

cells come from the same embryo and immortalization by serial passages requires a few dozen cell replications (Amand et al., 2016; Todaro and Green, 1963). Moreover, no mutations on NF-κB-related genes of the *wikipathways* database were identified.

Frequency of order relations for genes involved in the NF-κB pathway. We define the relative expression level of a gene in one of the clonal populations as its expression level divided by the average expression level across the clones B, R and G. By definition, for a given gene, the sum of their relative expression levels in clones R, G and B is always 3. For a given gene list we can calculate the relative expression value of each gene and then calculate the average value of the relative expression value of the gene list for each population and denote it as <R>, <G> and <B> respectively. It is easy to see that their sum has also to be equal to 3:

$$<R> + <G> + <B>=3$$

Hence, the average relative expression of two of the populations determine the value of the third. For a given gene list we can plot the average relative expression in just two dimensions, which for the sake of this paper we take as <R> and <B> (**Figures S4B**, **S4C**, **S5A**). Hence the average relative expression levels can be projected in the <R>-<B> plane. Choosing the average relative expression allows us to have a vision of the ensemble without giving a weight according to the average expression level of each gene. This appears reasonable since the proportionality between mRNA and protein might vary between genes.

There are six possible order relations between <R>, <G> and <B>, as for any three numbers. Hence average relative expression levels can adopt six different order relations. Each order relation determines a region in the 3-coordinate space <R> <G> <B>, each two regions are separated by a plane which intersects with the <R>-<B> plane giving a straight line. Hence, the <R>-<B> plane is divided in 6 sections that determine the 6 possible order relations between <R>, <G> and <B> (**Figures S4B**, **S4C**, **S5A**).

Here we calculate the average relative expression levels in three different gene lists:

TNF-α to NF-κB: *Tnfrsf1a, Tab2, Tab1, Traf2, Chuk, Tradd, Ikbkg, Ripk1, Ikbkb, Map3k7, Map3k3, Traf5, Fadd*.
IL-1β to NF-κB: *Tab2, Tab1, Myd88, Il1r1, Chuk, Ikbkg, Irak1, Ikbkb, Traf6, Map3k7, Irak4, Irak2, Il1rap, Irak3*
NF-κB negative feedback: *Nfkbia, Tnfaip3, Nfkbie, Nfkbib, Cyld.*

To assign a statistical significance to the order relations and the average relative expression values, we sampled across our RNA-seq data to find random gene sets with expression levels within the limits of those of the dataset considered (with values between the minimum and the maximum value of the gene set considered) and compute the probability of different average relative expression levels projected in the <R>-<B> plane (see **Figures S4B** for genes of the "TNF-α to NF-κB" list , **S4C** for genes of the "IL-1β to NF-κB" list and **S5A** for genes of the "NF-κB negative feedbacks" list). In each of them we also plot as a red dot the average relative expression values of the dataset considered, which of course falls in the section of the <R>-<B> plane that corresponds to the order relation obtained (**Figures S4B**, **S4C**, **S5A**).

bioRxiv preprint doi: https://doi.org/10.1101/2021.12.07.471485; this version posted December 9, 2021. The copyright holder for this preprint (which was not certified by peer review) is the author/funder, who has granted bioRxiv a license to display the preprint in perpetuity. It is made available under aCC-BY-NC-ND 4.0 International license.

Mathematical model of NF-κB signaling. Elaborating on previous models (Zambrano et al., 2014b, 2016) where the negative feedbacks were provided by the inhibitor IκBα and the A20 protein, we developed a more complete model in which the additional negative feedbacks specified in **Figure 5A** are taken into account.

In this new model, the amount of free nuclear NF-κB, N, depends on its continuous association-dissociation with the three IκB inhibitor proteins, whose amount we represent asI_i with $i = \{\alpha, \beta, \varepsilon\}$. They can indeed form the complex (cytosolic) forms $(N{:}\, I_i)$ for $i = \{\alpha, \beta, \varepsilon\}$. The equilibrium between forms is also dependent on the presence of the kinase IKK complex whose amount we denote as K. This means that:

$$\frac{dN}{dt} = \sum_{i=\alpha,\beta,\varepsilon} -k_{a,i} N \cdot I_i + k_{d,i} \cdot (N{:}\, I_i) + d_{C,i} \cdot (N{:}\, I_i) + d_{K,i} \cdot K \cdot (N{:}\, I_i)$$

Where $k_{a,i}$ and $k_{d,i}$ are the association and dissociation constants, respectively, while $d_{K,i}$ is the degradation rate of the complex due to the presence of the kinase complex and $d_{C,i}$ accounts for the spontaneous degradation of the complex. For each of the complex ($i = \{\alpha, \beta, \varepsilon\}$) we have that:

$$\frac{d(N{:}\, I_i)}{dt} = +k_{a,i} N \cdot I_i - k_{d,i} \cdot (N{:}\, I_i) - d_{C,i} \cdot (N{:}\, I_i) - d_{K,i} \cdot K \cdot (N{:}\, I_i)$$

For the inhibitors, beyond the association and dissociation processes of the complex, the evolution will depend also on the translation rate $k_{I,i}$ of the available mRNA of each of the three inhibitors, that we denote as R_i, and on the inhibitors own degradation rate $d_{I,i}$ and the kinase-dependent degradation rate $d_{IK,i}$:

$$\frac{dI_i}{dt} = -k_{a,i} N \cdot I_i + k_{d,i} \cdot (N{:}\, I_i) - d_{IK,i} \cdot K \cdot I_i + k_{I,i} \cdot R_i - d_{I,i} \cdot I_i$$

The amount of the kinase complex K is regulated by the amount of the protein A20, that we denote A, through a hill function of parameters A_0 and n, and will also depend on the degradation rate of the kinase complex d_K and the presence ($S = 1$) or absence ($S = 0$) of the external inflammatory signal and on the constant K_0

$$\frac{dK}{dt} = \frac{S \cdot K_0}{(1 + \left(\frac{A}{A_0}\right)^n)} - d_K \cdot K$$

The amount of A20 depends on the translation rate $k_{t,A}$ of the available mRNA, that we denote as R_A, and on the degradation rate d_A so:

bioRxiv preprint doi: https://doi.org/10.1101/2021.12.07.471485; this version posted December 9, 2021. The copyright holder for this preprint (which was not certified by peer review) is the author/funder, who has granted bioRxiv a license to display the preprint in perpetuity. It is made available under aCC-BY-NC-ND 4.0 International license.

$$\frac{dA}{dt} = k_{t,A} \cdot R_A - d_{\mathrm{A}} \cdot \mathrm{A}$$

The mRNA expression level of each repressor is encoded by the following equations:

$$\frac{dR_j}{dt} = k_j G_j - \delta_j R_j$$
$$\frac{dG_j}{dt} = k_{on,j} N \cdot (2 - G_j) - k_{off,j} G_j$$

Where $j = \{\alpha, \beta, \varepsilon, A\}$; A is the index representing A20. $G_j(t)$ represents the gene activity status for each of the negative feedbacks considered (number of "on" alleles) and $R_j(t)$ the mRNA levels. Concerning the parameters, δ_j is the degradation rate of the mRNA considered, k_j is the transcription rate, and $k_{on,j}$ and $k_{off,j}$ are the gene activation-inactivation rate for each of them. The starting parameters, largely based on those provided in (Zambrano et al., 2016) but further constrained by our experiments (see below) are provided in **Table S3**.

Integrating transcriptomics in mathematical modelling. In **Figure 5** we perform numerical simulations of NF-κB dynamics in clone B and clone R by generating random parameter sets so a) the ratios of the expression of the different IκB inhibitors within clones and b) the ratios of the expression of the expression of inhibitors between clones match the experimentally observed values. To do so, we proceed as follows. To assess the role of transcriptional differences we generate random sets of parameters that are varied up to 2-fold their original values, but we constrain them in such a way that the ratios of the expression of the inhibitors both within and between clones are preserved and match the experimentally observed ones. For the sake of simplicity and following what has been done by others (A.Hoffmann et al., 2002; Nelson et al., 2004), we assume that the parameters related with the gene activation do not vary between the genes encoding for the inhibitors. This implies that the RNA expression essentially depends only on the production and degradation rates of RNA k_i and δ_i. To further simplify things, we assume that the kinetics of mRNA degradation is similar between genes, so we keep δ_i constant for all the negative feedbacks. Hence, in our simulations, to make the ratios between the expression inhibitors within a clone match the ratios observed experimentally, we just need to tune the parameters k_i, i.e., the RNA production rate. For example, to generate a parameter set in such a way that in simulations the ratio between inhibitors expression values match the experimentally observed value $r_{\alpha,\beta}$, we randomly select the parameters k_α and δ_α and then impose that:

$$k_\beta = \frac{k_\alpha}{r_{\alpha,\beta}} \text{ keeping } \delta_\beta = \delta_\alpha .$$

Of note, this approach allows us to produce exactly the ratios of the inhibitors observed experimentally within a clone, as shown for example in **Figure 5E**. Similarly, to generate parameter sets for clone B and R where the relation expression levels of a given inhibitor satisfy the experimentally observed relation $r_{i,B\ vs\ R}$, we generate a random value for the transcription rate $k_{i,R}$ for clone R and impose that the transcription rate for clone B $k_{i,B}$ must be given by

bioRxiv preprint doi: https://doi.org/10.1101/2021.12.07.471485; this version posted December 9, 2021. The copyright holder for this preprint (which was not certified by peer review) is the author/funder, who has granted bioRxiv a license to display the preprint in perpetuity. It is made available under aCC-BY-NC-ND 4.0 International license.

$$r_{i,B\ vs\ R} = \frac{k_{i,B}}{k_{i,R}}$$

In particular, by generating randomly $k_{a,R}$ and considering the relations $r_{\alpha,\beta}$ and $r_{\alpha,\varepsilon}$for the amount of inhibitor transcript observed for each clone, with the experimentally determined relations $r_{\alpha,B\ vs\ R}$, $r_{\varepsilon,B\ vs\ R}$, $r_{\beta,B\ vs\ R}$ of inhibitor values between clones, we then impose transcription rates so the relations within (**Figure 5E**) and between clones (**Figure 5F**) are satisfied in the simulations performed in the randomly generated parameter sets. Of note, we also impose that the amount of p65 (NF-κB) for clone B must be close to 1.4-fold that of clone R (**Figure S4A**). Of note, this approach is not exact, and it only gives ratios between clones that are close to the imposed ones, but still we find that for most of the randomly generated parameters such differences are enough to produce differences in dynamics compatible with those experimentally observed.

Downmodulation of IκBα using antisense oligonucleotides. The antisense oligos to target the *Nfkbia* gene were designed by Aum Biotech, LLC (Philadelphia, PA, USA). Four custom antisense oligos in the final concentration of 5 μM were used to treat MEFs for 24 hours to reduce the expression of IκBα.

Statistical analysis. For all the statistical analysis not detailed above: non-parametric Kruskal-Wallis (for multiple comparisons) and Student's t-test were used as described in the figure captions. The threshold of significance was set to p=0.05.

bioRxiv preprint doi: https://doi.org/10.1101/2021.12.07.471485; this version posted December 9, 2021. The copyright holder for this preprint (which was not certified by peer review) is the author/funder, who has granted bioRxiv a license to display the preprint in perpetuity. It is made available under aCC-BY-NC-ND 4.0 International license.

REFERENCES

Adelaja, A., Taylor, B., Sheu, K.M., Liu, Y., Luecke, S., and Hoffmann, A. (2021). Six distinct NFκB signaling codons convey discrete information to distinguish stimuli and enable appropriate macrophage responses. Immunity 54, 916-930.e7.

Adetunji, M.O., Lamont, S.J., Abasht, B., and Schmidt, C.J. (2019). Variant analysis pipeline for accurate detection of genomic variants from transcriptome sequencing data. PLoS One 14, e0216838.

A.Hoffmann, Levchencko, A., Scott, M.L., and Baltimore, D. (2002). The IkappaB-NF-kappaB signalling module: temporal control and selective gene activation. Science 298, 1241–1245.

Alon, U. (2007). An Introduction to Systems Biology (Boca Raton, FL (USA): CRC Press).

Amand, M.M., Hanover, J.A., and Shiloach, J. (2016). A comparison of strategies for immortalizing mouse embryonic fibroblasts. Journal of Biological Methods 3, e41–e41.

Ankers, J.M., Awais, R., Jones, N.A., Boyd, J., Ryan, S., Adamson, A.D., Harper, C.V., Bridge, L., Spiller, D.G., Jackson, D.A., et al. (2016). Dynamic NF-κB and E2F interactions control the priority and timing of inflammatory signalling and cell proliferation. ELife 5, e10473.

Ashall, L., Horton, C.A., Nelson, D.E., Paszek, P., Harper, C.V., Sillitoe, K., Ryan, S., Spiller, D.G., Unitt, J.F., Broomhead, D.S., et al. (2009). Pulsatile Stimulation Determines Timing and Specificity of NF- B-Dependent Transcription. Science 324, 242–246.

Barken, D., Wang, C.J., Kearns, J., Cheong, R., Hoffmann, A., and Levchenko, A. (2005). Comment on "Oscillations in NF-κB Signaling Control the Dynamics of Gene Expression." Science 308, 52–52.

Beg, A.A., and Baltimore, D. (1996). An Essential Role for NF-κB in Preventing TNF-α-Induced Cell Death. Science 274, 782–784.

Brambilla, F., Garcia-Manteiga, J.M., Monteleone, E., Hoelzen, L., Zocchi, A., Agresti, A., and Bianchi, M.E. (2020). Nucleosomes effectively shield DNA from radiation damage in living cells. Nucleic Acids Research 48, 8993–9006.

Careccia, G., Colombo, F, Tirone, M, Agresti,A, Bianchi, ME, Zambrano, S, Vénéreau, E. (2019). Exploiting Live Imaging to Track Nuclei During Myoblast Differentiation and Fusion. Journal of Visualized Experiments : JoVE In press.

Cheng, Q.J., Ohta, S., Sheu, K.M., Spreafico, R., Adelaja, A., Taylor, B., and Hoffmann, A. (2021). NF-κB dynamics determine the stimulus specificity of epigenomic reprogramming in macrophages. Science 372, 1349–1353.

Cruz, J.A., Mokashi, C.S., Kowalczyk, G.J., Guo, Y., Zhang, Q., Gupta, S., Schipper, D.L., Smeal, S.W., and Lee, R.E.C. (2021). A variable-gain stochastic pooling motif mediates information transfer from receptor assemblies into NF-κB. Sci Adv 7, eabi9410.

De Lorenzi, R., Gareus, R., Fengler, S., and Pasparakis, M. (2009). GFP-p65 knock-in mice as a tool to study NF-κB dynamics in vivo. Genesis 47, 323–329.

DeFelice, M.M., Clark, H.R., Hughey, J.J., Maayan, I., Kudo, T., Gutschow, M.V., Covert, M.W., and Regot,

bioRxiv preprint doi: https://doi.org/10.1101/2021.12.07.471485; this version posted December 9, 2021. The copyright holder for this preprint (which was not certified by peer review) is the author/funder, who has granted bioRxiv a license to display the preprint in perpetuity. It is made available under aCC-BY-NC-ND 4.0 International license.

S. (2019). NF-κB signaling dynamics is controlled by a dose-sensing autoregulatory loop. Sci. Signal. 12.

Ferrell, J.E., Tsai, T.Y.-C., and Yang, Q. (2011). Modeling the Cell Cycle: Why Do Certain Circuits Oscillate? Cell 144, 874–885.

Franklin, J.M., Ghosh, R.P., Shi, Q., Reddick, M.P., and Liphardt, J.T. (2020). Concerted localization-resets precede YAP-dependent transcription. Nat Commun 11, 4581.

Gapuzan, M.-E.R., Schmah, O., Pollock, A.D., Hoffmann, A., and Gilmore, T.D. (2005). Immortalized fibroblasts from NF-kappaB RelA knockout mice show phenotypic heterogeneity and maintain increased sensitivity to tumor necrosis factor alpha after transformation by v-Ras. Oncogene 24, 6574–6583.

Greaves, M., and Maley, C.C. (2012). CLONAL EVOLUTION IN CANCER. Nature 481, 306–313.

Hayden, M.S., and Ghosh, S. (2008). Shared Principles in NF-kappaB Signaling. Cell 132, 344–344.

Kellogg, R., and Tay, S. (2015). Noise facilitates transcriptional control under dynamic inputs. Cell 160, 381–392.

Lane, K., Van Valen, D., DeFelice, M.M., Macklin, D.N., Kudo, T., Jaimovich, A., Carr, A., Meyer, T., Pe'er, D., Boutet, S.C., et al. (2017). Measuring Signaling and RNA-Seq in the Same Cell Links Gene Expression to Dynamic Patterns of NF-κB Activation. Cell Syst 4, 458-469.e5.

Lee, R.E., Walker, S.R., Savery, K., Frank, D.A., and Gaudet, S. (2014). Fold change of nuclear NF-kappaB determines TNF-induced transcription in single cells. Mol Cell 53, 867–879.

Lee, R.E.C., Qasaimeh, M.A., Xia, X., Juncker, D., and Gaudet, S. (2016). NF-κB signalling and cell fate decisions in response to a short pulse of tumour necrosis factor. Scientific Reports 6, 39519.

Lee, T.K., Denny, E.M., Sanghvi, J.C., Gaston, J.E., Maynard, N.D., Hughey, J.J., and Covert, M.W. (2009). A Noisy Paracrine Signal Determines the Cellular NF-kappaB response to Lipopolysaccharide. Science Signalling 2, 1–9.

Levine, J.H., Lin, Y., and Elowitz, M.B. (2013). Functional Roles of Pulsing in Genetic Circuits. Science 342, 1193–1193.

Li, Y., Shan, Y., Desai, R.V., Cox, K.H., Weinberger, L.S., and Takahashi, J.S. (2020). Noise-driven cellular heterogeneity in circadian periodicity. PNAS 117, 10350–10356.

Martin, E.W., Pacholewska, A., Patel, H., Dashora, H., and Sung, M.-H. (2020). Integrative analysis suggests cell type–specific decoding of NF-κB dynamics. Sci. Signal. 13.

Matsuda, M., Hayashi, H., Garcia-Ojalvo, J., Yoshioka-Kobayashi, K., Kageyama, R., Yamanaka, Y., Ikeya, M., Toguchida, J., Alev, C., and Ebisuya, M. (2020). Species-specific segmentation clock periods are due to differential biochemical reaction speeds. Science 369, 1450–1455.

McKenna, A., Hanna, M., Banks, E., Sivachenko, A., Cibulskis, K., Kernytsky, A., Garimella, K., Altshuler, D., Gabriel, S., Daly, M., et al. (2010). The Genome Analysis Toolkit: a MapReduce framework for analyzing next-generation DNA sequencing data. Genome Res 20, 1297–1303.

Milholland, B., Dong, X., Zhang, L., Hao, X., Suh, Y., and Vijg, J. (2017). Differences between germline and somatic mutation rates in humans and mice. Nat Commun 8, 15183.

bioRxiv preprint doi: https://doi.org/10.1101/2021.12.07.471485; this version posted December 9, 2021. The copyright holder for this preprint (which was not certified by peer review) is the author/funder, who has granted bioRxiv a license to display the preprint in perpetuity. It is made available under aCC-BY-NC-ND 4.0 International license.

Milo, R., and Phillips, R. (2015). Cell Biology by the Numbers (CRC Press.).

Natoli, G., and Ostuni, R. (2019). Adaptation and memory in immune responses. Nat Immunol 20, 783–792.

Nelson, D.E., Ihekwaba, A.E., Elliott, M., Johnson, J.R., Gibney, C.A., Foreman, B.E., Nelson, G., See, V., Horton, C.A., Spiller, D.G., et al. (2004). Oscillations in NF-kappaB signaling control the dynamics of gene expression. Science 306, 704–708.

Nelson, D.E., Horton, C.A., See, V., Johnson, J.R., Nelson, G., Spiller, D.G., Kell, D.B., and White, M.R.H. (2005). Response to Comment on "Oscillations in NF-κB Signaling Control the Dynamics of Gene Expression." Science 308, 52–52.

Paek, A.L., Liu, J.C., Loewer, A., Forrester, W.C., and Lahav, G. (2016). Cell-to-Cell Variation in p53 Dynamics Leads to Fractional Killing. Cell 165, 631–642.

Paszek, P., Ryan, S., Ashall, L., Sillitoe, K., Harper, C.V., Spiller, D.G., Rand, D.A., and White, M.R.H. (2010). Population robustness arising from cellular heterogeneity. Proc. Natl. Acad. Sci. USA 107, 11644–11649.

Patke, A., Young, M.W., and Axelrod, S. (2020). Molecular mechanisms and physiological importance of circadian rhythms. Nat Rev Mol Cell Biol 21, 67–84.

Purvis, J.E., and Lahav, G. (2013). Encoding and decoding cellular information through signaling dynamics. Cell 152, 945–956.

Purvis, J.E., Mock, K.W.K.C., Batchelor, E., Loewer, A., and Lahav, G. (2012). p53 Dynamics Control Cell Fate. Science 336, 1440–1444.

Schmitz, M.L., and Baeuerle, P.A. (1991). The p65 subunit is responsible for the strong transcription activating potential of NF-kappa B. The EMBO Journal 10, 3805–3817.

Schwanhäusser, B., Busse, D., Li, N., Dittmar, G., Schuchhardt, J., Wolf, J., Chen, W., and Selbach, M. (2011). Global quantification of mammalian gene expression control. Nature 473, 337–342.

Selimkhanov, J., Taylor, B., Yao, J., Pilko, A., Albeck, J., Hoffmann, A., Tsimring, L., and Wollman, R. (2014). Accurate information transmission through dynamic biochemical signaling networks. Science 346, 1370–1373.

Son, M., Wang, A.G., Tu, H.-L., Metzig, M.O., Patel, P., Husain, K., Lin, J., Murugan, A., Hoffmann, A., and Tay, S. (2021). NF-κB responds to absolute differences in cytokine concentrations. Sci. Signal. 14.

Sung, M.H., Salvatore, L., Lorenzi, R.D., Indrawan, A., Pasparakis, M., Hager, G.L., Bianchi, M.E., and Agresti, A. (2009). Sustained Oscillations of NF-kappaB Produce Distinct Genome Scanning and Gene Expression Profiles. PLoS ONE 5, e7163–e7163.

Sung, M.-H., Li, N., Lao, Q., Gottschalk, R.A., Hager, G.L., and Fraser, I.D.C. (2014). Switching of the Relative Dominance Between Feedback Mechanisms in Lipopolysaccharide-Induced NF-κB Signaling. Sci. Signal. 7, ra6–ra6.

Tay, S., Hughey, J.J., Lee, T.K., Lipniacki, T., Quake, S.R., and Covert, M.W. (2010). Single-cell NF-kappaB dynamics reveal digital activation and analogue information processing. Nature 466, 267–271.

bioRxiv preprint doi: https://doi.org/10.1101/2021.12.07.471485; this version posted December 9, 2021. The copyright holder for this preprint (which was not certified by peer review) is the author/funder, who has granted bioRxiv a license to display the preprint in perpetuity. It is made available under aCC-BY-NC-ND 4.0 International license.

Todaro, G.J., and Green, H. (1963). QUANTITATIVE STUDIES OF THE GROWTH OF MOUSE EMBRYO CELLS IN CULTURE AND THEIR DEVELOPMENT INTO ESTABLISHED LINES. J Cell Biol 17, 299–313.

Zambrano, S., Bianchi, M.E., and Agresti, A. (2014a). High-throughput analysis of NF-κB dynamics in single cells reveals basal nuclear localization of NF-κB and spontaneous activation of oscillations. PLoS ONE 9.

Zambrano, S., Bianchi, M.E., and Agresti, A. (2014b). A simple model of NF-κB dynamics reproduces experimental observations. Journal of Theoretical Biology 347.

Zambrano, S., de Toma, I., Piffer, A., Bianchi, M.E., and Agresti, A. (2016). NF-kappaB oscillations translate into functionally related patterns of gene expression. ELife 5, e09100–e09100.

Zambrano, S., Loffreda, A., Carelli, E., Stefanelli, G., Colombo, F., Bertrand, E., Tacchetti, C., Agresti, A., Bianchi, M.E., Molina, N., et al. (2020). First Responders Shape a Prompt and Sharp NF-κB-Mediated Transcriptional Response to TNF-α. IScience 23, 101529.

Zhang, Q., Gupta, S., Schipper, D.L., Kowalczyk, G.J., Mancini, A.E., Faeder, J.R., and Lee, R.E.C. (2017a). NF-κB dynamics discriminate between TNF doses in single cells. Cell Syst 5, 638-645.e5.

Zhang, Z.-B., Wang, Q.-Y., Ke, Y.-X., Liu, S.-Y., Ju, J.-Q., Lim, W.A., Tang, C., and Wei, P. (2017b). Design of Tunable Oscillatory Dynamics in a Synthetic NF-κB Signaling Circuit. Cell Systems 5, 460-470.e5.